



Wenhao Chen · Xu Liang · Shengping Shen

# Forced vibration of piezoelectric and flexoelectric Euler–Bernoulli beams by dynamic Green’s functions

Received: 4 July 2020 / Revised: 1 October 2020 / Accepted: 15 October 2020 / Published online: 17 November 2020  
© Springer-Verlag GmbH Austria, part of Springer Nature 2020

**Abstract** This work presents the dynamic response of piezoelectric and flexoelectric Euler–Bernoulli beams subjected to mechanical loads by means of Green’s functions. Exact solutions in closed form for the electromechanical coupling behaviors are derived. The present solutions will reduce to those of classical piezoelectric beam models by neglecting the flexoelectric effect. Numerical results for a BaTiO<sub>3</sub> cantilever show that the tip deflection of the beam will be separated when the beam thickness reduces to one micrometer; therefore, pure mechanical experiments can be used to determine the flexoelectric effect by a bending test under different electrical boundary conditions. In addition, the dynamic output voltage under open-circuit condition and the dynamic output charge under short-circuit condition are dominated by the flexoelectric effect. The dynamic output voltage and charge become negligible when the beam thickness reduces to one micrometer. By reducing the length–thickness ratio or introducing the effective piezoelectric coefficient, the electric response can be more easily detected at microscale. These results demonstrate that the flexoelectric effect can be strong enough to dominate the electromechanical coupling behavior, coordinating with the ‘ever green’ trend to miniaturization, and the flexoelectric effect can be applicable for energy harvesters, sensing, and others.

## 1 Introduction

The rapid development of microelectromechanical systems (MEMS) and nanoelectromechanical systems (NEMS) in the past decades has been fueled by the fast growth of the nanotechnology. Piezoelectric elements such as beams, plates and shells have been widely utilized as the building blocks in the MEMS and NEMS as sensors, actuators, and others [1]. Flexoelectric elements are the other promising building blocks in the next-generation MEMS and NEMS devices [2–5], besides of the state-of-the-art piezoelectric devices. Unlike piezoelectricity, flexoelectricity is a universal electromechanical coupling which exists in all dielectrics due to the local inversion symmetry breaking by the strain gradient. Unexpectedly, the flexoelectric coefficients for certain perovskite ferroelectrics such as lead magnesium niobate (PMN) [6], barium strontium titanate (BST) [7], lead zirconate titanate (PZT) [8], and barium titanate (BT) [9] are three to five orders magnitude larger than those of the theoretical predictions [10, 11] and first-principle calculations [12, 13]. These experiment results triggered the investigation of flexoelectricity in the fundamental mechanical elements.

From the continuum mechanics point of view, the strain gradient elasticity is considered as a higher-order gradient theory. The study of higher-order strain gradient elasticity and couple stress theory can be traced back

---

W. Chen · X. Liang · S. Shen  
State Key Laboratory for Strength and Vibration of Mechanical Structures, School of Aerospace Engineering,  
Xi’an Jiaotong University, Xi’an 710049, China

X. Liang (✉) · S. Shen  
Shaanxi Key Laboratory for Vibration and Control of Aerospace Structures, School of Aerospace Engineering,  
Xi’an Jiaotong University, Xi’an 710049, China  
E-mail: xliang226@xjtu.edu.cn

to the work of Mindlin [14], Mindlin and Eshel [15], and Toupin [16]. Later, the study of higher-order gradient and generalized continua mechanics goes back to the nonlocal elastic theory by Eringen [17, 18]. The theory of flexoelectricity for elastic dielectrics can be considered as a higher-order electromechanical coupling theory. The origin of the elastic dielectrics with flexoelectricity might be found in the earlier work of Mindlin [19], in which the polarization gradient has been involved in the framework of the continuum elastic dielectrics. Sharma and co-workers [20], and Cross and co-workers proposed a modified phenomenological model for the flexoelectric effects in solid dielectrics. Sharma and co-workers [21–24] have extended Mindlin's work by including the strain gradient terms. In Cross's work, the flexoelectric effects have been investigated from the viewpoint of equilibrium thermodynamics. The physical fundamental of the flexoelectricity for elastic dielectrics can be found in Shen and Hu [25–27], in which the electrostatic force, surface piezoelectric and flexoelectric effect were all take into consideration in the continuum theoretical frameworks.

Based on the above-mentioned continuum theoretical frameworks, Jiang and co-workers [28–30] investigated the static bending and vibration of piezoelectric nanobeams with flexoelectricity. Liang et al [31–33] studied the static bending, buckling, and vibration behaviors of piezoelectric nanostructures with consideration of the surface and flexoelectric effect. The electromechanical response of piezoelectric nanostructures and flexoelectric nanostructures can be also found in various previous works [34–36]. Further, flexoelectricity has been verified to play an important role in the magnetoelectric behaviors of a multiferroic composite, which provides a novel notion for designing multiferroic devices [37, 38]. The forced vibration of piezoelectric and flexoelectric beams due to steady loads is a very important issue in engineering applications. However, exact solutions for the forced vibration of piezoelectric and flexoelectric Euler–Bernoulli beams (EBs) are still limited. As pointed out by the previous investigation, the static measurement offers only a rough estimation of the flexoelectric effect, and it is generally inaccurate in comparison to dynamic measurements [39]. The forced vibration of Euler–Bernoulli beams (EBs) and Timoshenko beams (TBs) has been rigorously studied by means of the Green's functions [40, 41]. In the light of the dynamic experimental measurement of the flexoelectric coefficient for perovskite ceramics and polymer materials [42–45], it is essential to present the dynamic response of piezoelectric and flexoelectric beams. To the author's knowledge, mechanical structural design and functionally graded composite can greatly enhance the electromechanical behaviors of dielectrics, leading to a higher performance and a wider range of application in energy conversion devices [46–49]. Here we propose a novel way based on the size-dependent electromechanical couplings to fabricate BT-based materials with ultrahigh piezoelectric coefficient, which can be a guideline for designing new flexoelectric devices.

## 2 Piezoelectric and flexoelectric Euler–Bernoulli beams

In order to simplify the discussion, the higher-order gradients terms (fifth and sixth strain gradient terms) are neglected. The electric enthalpy in considering both the piezoelectric and flexoelectric effects can be written as [50, 51]

$$H = -\frac{1}{2}a_{kl}E_kE_l + \frac{1}{2}c_{ijkl}\varepsilon_{ij}\varepsilon_{kl} - e_{ijk}\varepsilon_{ij}E_k - \mu_{ijkl}E_k\varepsilon_{ij,l} \quad (1)$$

where  $a_{ij}$  and  $c_{ijkl}$  are the second-rank dielectric constant and elastic stiffness constant, respectively. In addition,  $e_{ijk}$  is the third-rank piezoelectric constant, while  $\mu_{ijkl}$  is the fourth-rank flexoelectric constant.

The displacement components for EBs can be written as

$$u(x, y, z, t) = -z \frac{\partial w_0}{\partial x}, \quad v(x, y, z, t) = 0, \quad w(x, y, z, t) = w_0(x, t) \quad (2)$$

where  $w_0(x, t)$  is the deflection of the neutral plane.

The elastic strains can be then derived from Eq. (2) from the displacement–strain relation as

$$\varepsilon_{xx} = \frac{\partial u}{\partial x} = -z \frac{\partial^2 w_0}{\partial x^2}. \quad (3)$$

The only nontrivial gradients of strain are

$$\eta_{xxx} = \frac{\partial \varepsilon_{xx}}{\partial x} = -z \frac{\partial^3 w_0}{\partial x^3}, \quad \eta_{zxx} = \frac{\partial \varepsilon_{xx}}{\partial z} = -\frac{\partial^2 w_0}{\partial x^2}. \quad (4)$$

For a flexoelectric beam with electrodes on its top and bottom surfaces, the electric field is assumed in the thickness direction, as pointed out in our previous works [32]. The electric potential is assumed in the form as  $\varphi = \varphi(z, t)$ ; therefore, the electric field can be written as  $E_z(z, t) = -\partial\varphi/\partial z$ .

From Eq. (1), the constitutive equation for the piezoelectric EBs with flexoelectric effect can be written as

$$\sigma_{xx} = c_{11}\varepsilon_{xx} - e_{31}E_z, \quad \tau_{zxx} = -\mu_{31}E_z. \quad (5)$$

And the electric displacement and higher-order electric displacement are

$$D_z = a_{33}E_z + e_{31}\varepsilon_{xx} + \mu_{31}\eta_{zxx}. \quad (6)$$

In case of open-circuit condition, the electric displacement on the surface is zero,  $D_z|_a = 0$ . And considering the Gauss's Law of the electric displacement,  $\partial D_z/\partial z = 0$ , one gets that the electric displacement should be equal to zero. Thus, from Eq. (6) one gets

$$E_z = -\frac{e_{31}}{a_{33}}\varepsilon_{xx} - \frac{\mu_{31}}{a_{33}}\eta_{zxx}. \quad (7)$$

Then, substituting Eq. (7) into Eq. (5) yields

$$\begin{aligned} \sigma_{xx} &= \left(c_{11} + \frac{e_{31}^2}{a_{33}}\right)\varepsilon_{xx} + \frac{e_{31}\mu_{31}}{a_{33}}\eta_{zxx}, \\ \tau_{zxx} &= \frac{e_{31}\mu_{31}}{a_{33}}\varepsilon_{xx} + \frac{\mu_{31}^2}{a_{33}}\eta_{zxx}. \end{aligned} \quad (8)$$

The equilibrium equations and boundary conditions of the beam can then be derived from Hamilton's principle [52],

$$\delta \int_{t_1}^{t_2} L dt + \int_{t_1}^{t_2} \delta W dt = 0, \quad (9)$$

where  $L$  is the Lagrange density defined by

$$L = \int_V \left( \frac{1}{2} \rho \dot{u}_i \dot{u}_i - H \right) dV \quad (10)$$

As pointed out by Tiersten [52], the Lagrange density in Eq. (10) is the kinetic energy minus the electric enthalpy as in piezoelectric media, rather than the kinetic energy minus the internal energy as in pure elasticity. The work done by the external force  $p(x, t)$  can be expressed as

$$W = \int_0^L P(x, t) w_0(x, t) dx. \quad (11)$$

Substituting Eqs. (2), (8), and (11) into Eq. (9) gives

$$\begin{aligned} &\delta \int_{t_1}^{t_2} L dt + \int_{t_1}^{t_2} \delta W dt \\ &= \int_{t_1}^{t_2} dt \int_V (\rho \dot{w}_0 \delta \dot{w}_0 - \sigma_{xx} \delta \varepsilon_{xx} - \tau_{zxx} \delta \eta_{zxx}) dV + \int_{t_1}^{t_2} dt \int_0^L p(x, t) \delta w_0(x, t) dx \\ &= \int_{t_1}^{t_2} \left[ (M + P) \delta \left( \frac{\partial w_0}{\partial x} \right) \right]_0^L dt - \int_{t_1}^{t_2} \left[ \left( \frac{\partial (M + P)}{\partial x} \right) \delta w_0 \right]_0^L dt \\ &\quad + \int_{t_1}^{t_2} dt \int_0^L \left[ \frac{\partial^2 (M + P)}{\partial x^2} - \rho A \ddot{w}_0 + p(x, t) \right] \delta w_0 dx \end{aligned} \quad (12)$$

where  $M$  and  $P$  are the bending moment and higher-order bending moment on the cross section, respectively. These internal generalized forces are defined by

$$M(x) = - \left( c_{11} + \frac{e_{31}^2}{a_{33}} \right) I \frac{\partial^2 w_0}{\partial x^2}, \quad P = - \frac{\mu_{31}^2 A}{a_{33}} \frac{\partial^2 w_0}{\partial x^2}. \quad (13)$$

Due to the arbitrariness of  $\delta w_0$ , the governing equations for the piezoelectric and flexoelectric EBs are

$$\frac{\partial^2 M}{\partial x^2} + \frac{\partial^2 P}{\partial x^2} - \rho A \ddot{w}_0 + p(x, t) = 0. \quad (14)$$

And the corresponding boundary conditions for a cantilever beam are

$$\begin{aligned} w_0(x=0) &= 0, \quad \left[ \frac{\partial M}{\partial x} + \frac{\partial P}{\partial x} \right] \Big|_{x=L} = 0, \\ \frac{\partial w_0}{\partial x} \Big|_{x=0} &= 0, \quad (M + P) \Big|_{x=L} = 0. \end{aligned} \quad (15)$$

By substituting Eq. (13) into Eq. (14), one gets the governing equations expressed by displacement  $w_0$  as

$$\frac{\partial^4 w_0}{\partial x^4} + \frac{\rho A}{(EI)^{\text{eff}}} \ddot{w}_0 = \frac{1}{(EI)^{\text{eff}}} p(x, t) \quad (16)$$

where  $(EI)^{\text{eff}}$  is the effective bending rigidity, defined by

$$(EI)^{\text{eff}} = \left( c_{11} + \frac{e_{31}^2}{a_{33}} \right) I + \frac{\mu_{31}^2 A}{a_{33}}, \quad (17)$$

In the case of the short-circuit condition, the electric field  $E_z(x, t)$  is equal to zero. Hence, the higher-order couple stresses vanish. Equation (5) reduces to  $\sigma_{xx} = c_{11} \varepsilon_{xx}$ .

The explicit governing equations are then reduced to

$$c_{11} I \frac{\partial^4 w_0}{\partial x^4} + \rho A \ddot{w}_0 = p(x, t). \quad (18)$$

Under this condition, the governing equations reduce to the same form as the classical EBs without electromechanical coupling. However, the electric charge on the upper and lower surface can be detected to measure the flexoelectric coefficient,

$$D_z = e_{31} \varepsilon_{xx} + \mu_{31} \eta_{xxz}. \quad (19)$$

When the electric charge on the surface is detected, then one has

$$\Delta Q = \frac{Q^{\text{upper}} - Q^{\text{lower}}}{2} = \mu_{31} A_e \frac{\partial^2 w_0}{\partial x^2} \quad (20)$$

where  $Q^{\text{upper}}$  and  $Q^{\text{lower}}$  have the same magnitude but with opposite sign because of the pure bending state, and  $A_e$  is the area of the electrode on the upper and lower surface. When the tip displacement of cantilever beams is detected, the expression of the displacement can be expressed by the tip displacement so that the flexoelectric coefficient can be determined by Eq. (20); the schematic graph for measuring the flexoelectric coefficient is shown in Fig. 1a. It should be noticed that the detected electric charge is contributed to only the flexoelectric effect. Figure 1b displays that the upper part of the beam is in opposite mechanical state with the lower part of the beam; therefore, the electric charge induced by the piezoelectric effect has the same sign on both the upper and lower surfaces. There is no current flow in the circuit under short-circuit condition. However, flexoelectric effect-induced bound charge has opposite sign on the upper and lower electrodes; therefore, weak electric current should be detected. Similarly, piezoelectricity doesn't contribute to the electric potential, which will be discussed in detail in the following Sections. The elimination of the piezoelectric effect in pure bending leads to the measurement of the flexoelectric effect practically.

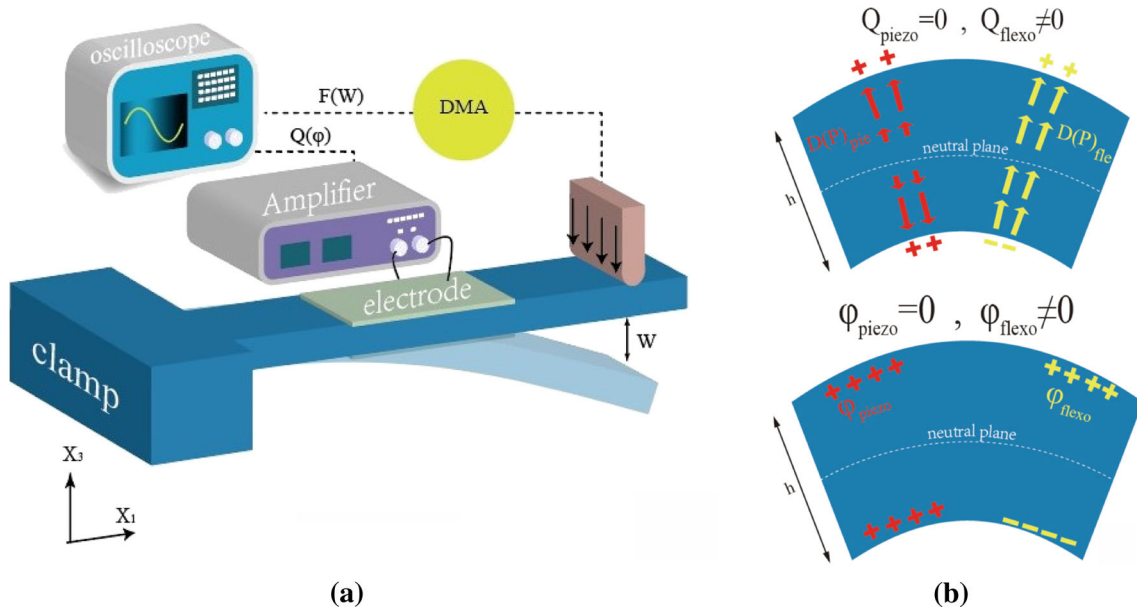


**Fig. 1** **a** Experiment arrangement for the measurement of flexoelectric coefficient; **b** illustration of the electric response under short-circuit condition and open-circuit condition. The polarization direction is given by the arrows (red for piezoelectric effect, yellow for flexoelectric effect)

### 3 Green's function solutions for the forced vibration

In order to obtain the analytical solution for the forced vibration of piezoelectric and flexoelectric EBs, we use the Green's function. Considering the piezoelectric and flexoelectric EBs excited by a harmonic force, then, the method of separation of variables and the synchronous motion hypothesis give

$$\begin{aligned} p(x, t) &= P(x)e^{i\omega t}, \\ w_0(x, t) &= W(x)e^{i\omega t}. \end{aligned} \quad (21)$$

By substituting Eqs. (21) into the governing Eqs. (16), one gets the governing equations for the piezoelectric and flexoelectric EBs with open-circuit condition as

$$W^{(4)}(x) - a_1 W(x) = b_1 P(x) \quad (22)$$

where  $a_1 = \rho A \omega^2 / (EI)^{\text{eff}}$ ,  $b_1 = 1 / (EI)^{\text{eff}}$ .

If the flexoelectric effect is neglected, letting  $\mu_{31} = 0$ , the governing equation (22) reduces to that of the classical piezoelectric Euler–Bernoulli beam model with effective bending rigidity  $(EI)^{\text{eff}} = c_{11} + e_{31}^2 / a_{33}$ . Note that the external force has an opposite direction in our model compared with that in Ref. [41]. We focus on the electromechanical coupling behaviors so that we do not try to deal with the damping effect in our work. And the definition of the effective bending rigidity for EB under various physical conditions can also be found in our previous works [32, 33, 53, 54].

To obtain the solution for the governing equation (22) with the superposition principle, we present the transverse displacement  $W(x)$  as an integral equation of a Green's function as

$$W(x) = \int_0^L P(x_0) G(x, x_0) dx \quad (23)$$

where the Green's function  $G(x, x_0)$  means its response of a unit concentrated force acting at an arbitrary position  $x_0$ , and  $P(x_0)$  is the amplitude of the external force.

First we consider an unit concentrated force applied at an arbitrary position  $x_0$ , i.e.,  $P(x) = \delta(x - x_0)$ ; then, Eq. (23) can be expressed as  $W(x) = G(x, x_0)$ . And mathematically,  $G(x, x_0)$  is the solution of the following equation:

$$G^{(4)} - a_1 G = b_1 \delta(x - x_0). \quad (24)$$

After using the Laplace transform method with respect to the variable  $x$ , the Green's function can be expressed as

$$\hat{G}(s, x_0) = \frac{R(s)}{s^4 - a_1}. \quad (25)$$

The characteristic equation of Eq. (24) has the form

$$s^4 - a_1 = 0. \quad (26)$$

The roots of Eq. (26) are

$$s_1 = a_1^{1/4}, \quad s_2 = -a_1^{1/4}, \quad s_3 = ia_1^{1/4}, \quad s_4 = -ia_1^{1/4}. \quad (27)$$

This gives the solution in the form of

$$\hat{G}(s, x_0) = \frac{R(s)}{(s - s_1)(s - s_2)(s - s_3)(s - s_4)}. \quad (28)$$

The inverse transform of  $\hat{G}(s, x_0)$  gives

$$\begin{aligned} G(x, x_0) = & H(x - x_0)\Phi_1(x - x_0) + \Phi_2(x)G(0) \\ & + \Phi_3(x)G^{(1)}(0) + \Phi_4(x)G^{(2)}(0) + \Phi_5(x)G^{(3)}(0) \end{aligned} \quad (29)$$

where  $\Phi_i$  ( $i = 1, 2, \dots, 5$ ) are defined by

$$\begin{aligned} \Phi_1(x - x_0) = & \sum_{i=1}^4 b_1 A_i(x - x_0), \quad \Phi_2 = \sum_{i=1}^4 A_i(x)(s_i^3 + a_1 s_i), \\ \Phi_3 = & \sum_{i=1}^4 A_i(x)(s_i^2 + a_1), \quad \Phi_4 = \sum_{i=1}^4 A_i(x)s_i, \quad \Phi_5 = \sum_{i=1}^4 A_i(x). \end{aligned} \quad (30)$$

Where  $A_i$  ( $i = 1, 2, \dots, 4$ ) are functions given by

$$\begin{aligned} A_1(x) = & \frac{e^{s_1 x}}{(s_1 - s_2)(s_1 - s_3)(s_1 - s_4)}, \quad A_2(x) = \frac{e^{s_2 x}}{(s_1 - s_2)(s_3 - s_2)(s_4 - s_2)}, \\ A_3(x) = & \frac{e^{s_3 x}}{(s_3 - s_1)(s_3 - s_2)(s_3 - s_4)}, \quad A_4(x) = \frac{e^{s_4 x}}{(s_4 - s_1)(s_4 - s_2)(s_4 - s_3)}. \end{aligned} \quad (31)$$

#### 4 Determination of the constants by boundary conditions

Various derivatives of  $G(x, x_0)$  can be derived from Eq. (29) as

$$\begin{aligned} G^{(1)}(x, x_0) = & \Phi_1^{(1)}(x - x_0) + \Phi_2^{(1)}(x)G(0) \\ & + \Phi_3^{(1)}(x)G^{(1)}(0) + \Phi_4^{(1)}(x)G^{(2)}(0) + \Phi_5^{(1)}(x)G^{(3)}(0), \end{aligned} \quad (32)$$

$$\begin{aligned} G^{(2)}(x, x_0) = & \Phi_1^{(2)}(x - x_0) + \Phi_2^{(2)}(x)G(0) \\ & + \Phi_3^{(2)}(x)G^{(1)}(0) + \Phi_4^{(2)}(x)G^{(2)}(0) + \Phi_5^{(2)}(x)G^{(3)}(0), \end{aligned} \quad (33)$$

$$\begin{aligned} G^{(3)}(x, x_0) = & \Phi_1^{(3)}(x - x_0) + \Phi_2^{(3)}(x)G(0) \\ & + \Phi_3^{(3)}(x)G^{(1)}(0) + \Phi_4^{(3)}(x)G^{(2)}(0) + \Phi_5^{(3)}(x)G^{(3)}(0). \end{aligned} \quad (34)$$

**Table 1** Boundary conditions of the piezoelectric and flexoelectric cantilever beam

Boundary conditions	Clamped	Free
Cantilever beam	$G(0) = 0$ $G^{(1)}(0) = 0$	$G^{(2)}(L) = 0$ $G^{(3)}(L) = 0$

Equations (29), (32–34) establish the relations between the quantities at arbitrary cross section  $x$ . Particularly, at the boundary  $x = L$ , one gets

$$\begin{bmatrix} \Phi_2(L) & \Phi_3(L) & \Phi_4(L) & \Phi_5(L) \\ \Phi_2^{(1)}(L) & \Phi_3^{(1)}(L) & \Phi_4^{(1)}(L) & \Phi_5^{(1)}(L) \\ \Phi_2^{(2)}(L) & \Phi_3^{(2)}(L) & \Phi_4^{(2)}(L) & \Phi_5^{(2)}(L) \\ \Phi_2^{(3)}(L) & \Phi_3^{(3)}(L) & \Phi_4^{(3)}(L) & \Phi_5^{(3)}(L) \end{bmatrix} \begin{Bmatrix} G(0) \\ G^{(1)}(0) \\ G^{(2)}(0) \\ G^{(3)}(0) \end{Bmatrix} = \begin{Bmatrix} G(L, x_0) - \Phi_1(L - x_0) \\ G^{(1)}(L, x_0) - \Phi_1^{(1)}(L - x_0) \\ G^{(2)}(L, x_0) - \Phi_1^{(2)}(L - x_0) \\ G^{(3)}(L, x_0) - \Phi_1^{(3)}(L - x_0) \end{Bmatrix}. \tag{35}$$

By setting  $\Phi_1 = 0$ , one obtains the free vibration of the piezoelectric and flexoelectric Euler–Bernoulli beam. The constants  $G(0)$ ,  $G^{(1)}(0)$ ,  $G^{(2)}(0)$ , and  $G^{(3)}(0)$  can be determined by the corresponding boundary conditions. For a cantilever beam which is clamped at  $x = 0$  and free at  $x = L$ , the corresponding boundary conditions are given in Eqs. (15). The boundary conditions then can be rewritten by the Green’s function  $G(x, x_0)$  as shown in Table 1.

With the boundary conditions in Table 1 and relations in Eqs. (35), one can obtain

$$\begin{bmatrix} \Phi_4^{(2)}(L) & \Phi_5^{(2)}(L) \\ \Phi_4^{(3)}(L) & \Phi_5^{(3)}(L) \end{bmatrix} \begin{Bmatrix} G^{(2)}(0) \\ G^{(3)}(0) \end{Bmatrix} = \begin{Bmatrix} -\Phi_1^{(2)}(L - x_0) \\ -\Phi_1^{(3)}(L - x_0) \end{Bmatrix}. \tag{36}$$

Thus, Green’s function for the cantilever EB is determined as

$$G(x, x_0) = H(x - x_0)\Phi_1(x - x_0) + \Phi_4(x)G^{(2)}(0) + \Phi_5(x)G^{(3)}(0). \tag{37}$$

Then, the explicit expression of the transverse displacement excited by a unit harmonic force can be written as

$$w(x, t) = \left[ H(x - x_0)\Phi_1(x - x_0) + \Phi_4(x)G^{(2)}(0) + \Phi_5(x)G^{(3)}(0) \right] \sin \omega t \tag{38}$$

where  $\omega = 2\pi f$  is the circular frequency of the external excited force.

After obtaining the dynamic mechanical response of EB, we can gain the output charge under short-circuit condition and output voltage under open circuit. Under open-circuit condition, the total electric displacement on the top and bottom surface is zero. Thus,

$$\int_{S_e} (a_{33}E_3 + e_{31}\varepsilon_{11} + \mu_{31}\partial_3\varepsilon_{11})dS = 0. \tag{39}$$

With the help of the Green’s function  $G(x, x_0)$ , the average electric field can be written as

$$\bar{E}_3(x, t) = \frac{1}{a_{33}S_e} \int_{S_e} \left[ e_{31}zG^{(2)}(x, x_0) + \mu_{31}G^{(2)}(x, x_0) \right] dS. \tag{40}$$

The dynamic output of the electric potential can be written as

$$\varphi(t) = - \int_{-\frac{h}{2}}^{\frac{h}{2}} E_z dz \sin \omega t = - \frac{\mu_{31}}{a_{33}S_e/Bh} \int_0^L G^{(2)}(x, x_0)dx \sin \omega t. \tag{41}$$

It should be noticed that the electric potential induced by piezoelectricity is zero because of the symmetry through thickness. Thus, only flexoelectricity contributes to the dynamic output of the electric potential, as shown in Fig. 1b.

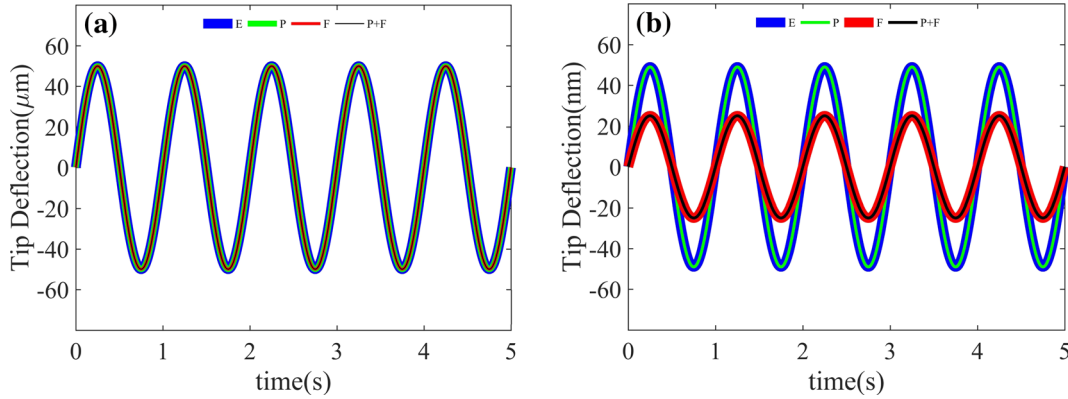


**Fig. 2** Dynamic deflection of the beam versus time at  $x = L$ , **a**  $H = 1$  mm; **b**  $H = 1$   $\mu$ m

Under short circuit, the electric field along the thickness is zero; thus, the electric displacement can be written as

$$D_3 = (e_{31}\varepsilon_{11} + \mu_{31}\partial_3\varepsilon_{11}) \sin \omega t. \quad (42)$$

Then, the output charge along the thickness of the beam can be written as

$$Q(t) = \frac{1}{h} \int_V D_3 dV = -\mu_{31} B \int_0^L G^{(2)}(x, x_0) dx \sin \omega t. \quad (43)$$

## 5 Numerical results and discussion

Considering a unit force loaded at the free end of the cantilever beam, the external force can be expressed as  $p(x, t) = \delta(x - L)e^{i\omega t}$ . The width–thickness ratio is taken  $b = 2h$ . We introduce the following dimensionless quantities:

$$\xi = \frac{x}{L}, \quad \beta = \frac{h}{L}, \quad g(\xi) = \frac{G(x, L)}{w_{\max}}. \quad (44)$$

Material properties in the numerical calculations are chosen as  $c_{11} = 108$  GPa,  $a_{33} = 1.12 \times 10^{-8}$  F/m,  $e_{31} = -4.4$  C/m<sup>2</sup>,  $\mu_{31} = 10$   $\mu$ C/m [9], and  $\rho = 5780$  kg/m<sup>3</sup>.

The static solution for the deflection of the beam is

$$w(x) = \frac{F(x - 3L)x^2}{6(EI)^{\text{eff}}}. \quad (45)$$

To maintain the elastic deformation, we choose  $F = \frac{Eb^4}{80L^3}$ .

In this Section, we consider the forced vibration of the Euler–Bernoulli piezoelectric and flexoelectric beam driven by a unit force loaded at the free end of the cantilever beam; therefore, the deflection of the beam can be expressed by the Green's function  $G(x, L)$ .

When considering  $\beta = 20$ ,  $f = 1$  Hz, the dynamic deflection of the beam versus time at the position  $x = L$  is illustrated in Fig. 2. 'E', 'P', 'F', and 'P+F' in Fig. 2 represents elastic beam, piezoelectric beam, flexoelectric beam, and piezoelectric and flexoelectric beam, respectively. In Fig. 2a, the applied force is about 0.3 N, and the thickness of the beam is one millimeter. It is obvious that the dynamic deflection of the elastic beam, piezoelectric beam, flexoelectric beam, and piezoelectric and flexoelectric beam almost equal each other. This implies that the effect of piezoelectricity, flexoelectricity or both does not affect the dynamic deflection significantly at the macroscopic level. However, the dynamic deflection of the elastic beam, piezoelectric beam, flexoelectric beam, and piezoelectric and flexoelectric beam is separated when the thickness of the cantilever beam reduces to ten micrometer, as shown in Fig. 2b. The applied force is about 0.3  $\mu$ N to maintain the beam in elastic deformation. Therefore, the elastic strain is almost in the same level in Fig. 2a, b. The elastic strain gradient is, however, inversely proportional to the beam thickness. The elastic strain gradient in Fig. 2b is



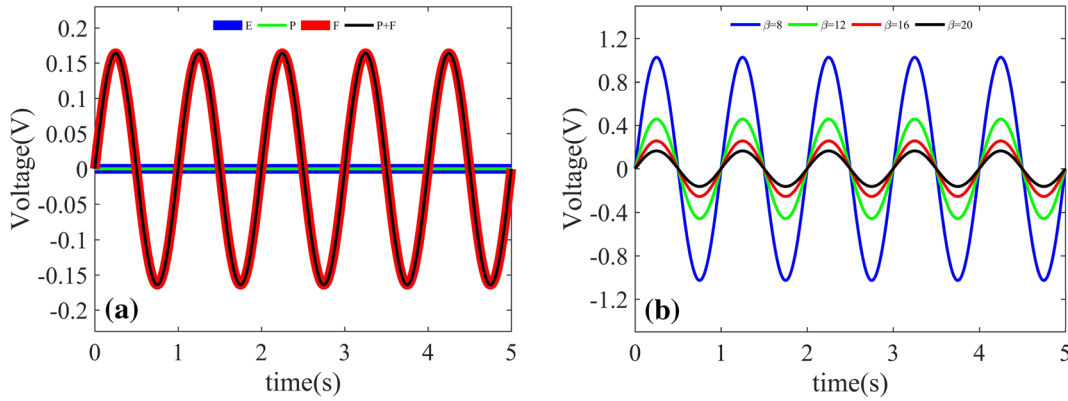


**Fig. 3** Dynamic output voltage versus time **a**  $H = 1 \text{ mm} \sim 10 \mu\text{m}$ ; **b** different length–thickness ratios when  $H = 1 \text{ mm}$

much larger than that in Fig. 2a. The dynamic deflection of the elastic beam is equal to that of the piezoelectric beam in Fig. 2b, while the dynamic deflection of the flexoelectric beam is smaller than that of the elastic and piezoelectric beam. Moreover, the dynamic deflection of the flexoelectric beam is equal to that of the piezoelectric and flexoelectric beam. Therefore, Fig. 2b reveals that the difference in the dynamic deflection could be ascribed to the effect of flexoelectricity. The results in Fig. 2 imply that the effect of flexoelectricity becomes significant when the beam thickness reduces to microscale. For short-circuit condition, however, the effects of piezoelectricity and flexoelectricity do not affect the dynamic deflection because the elastic modulus remains constant. As a result, one may determine the flexoelectric coefficient for beams by a pure elastic technique at the microscale, such as testing the bending rigidity of the beam or determining the dynamic deflection of the flexoelectric beam under open-circuit condition.

The dynamic output voltage versus time of the Euler–Bernoulli beam is illustrated in Fig. 3. Obviously, elastic and piezoelectric Euler–Bernoulli beam will not cause any output voltage, owing to the tensile state of the upper part in the beam while the compressive state is in the lower part of the beam, as displayed in Fig. 1b. The flexoelectric Euler–Bernoulli beam, however, will cause output voltage due to the flexoelectric effect.

We find that the peak voltage for a flexoelectric Euler–Bernoulli beam is 0.164 V, and this value remains almost constant when the beam thickness reduces to fifty micrometers. This can be explained via the static solution of the output voltage, which can be expressed as

$$\varphi = \frac{3\mu_{31}}{40a_{33}\beta^2}. \quad (46)$$

The dynamic output voltage for a flexoelectric Euler–Bernoulli beam will be increasingly remarkable when the length–thickness ratio  $\beta$  decreases (Fig. 3b). The results above throw light on enhancing the dynamic output voltage by changing the size of the beam, besides increasing the intrinsic flexoelectric coefficient.

Moreover, these results lead us to rethink some of the existing works [55–57]. In these works, BaTiO<sub>3</sub> nanowires or nanowire arrays were used to harvest energy from the environmental vibration. The flexible nanogenerator based on single BaTiO<sub>3</sub> nanowire can generate an output voltage of up to 0.21 V and has been found in the previous works [57]. Our results imply that the flexoelectric effect might play an important role in the dynamic output voltage of the nanogenerators.

Figure 4a illustrates the dynamic output charge versus time under short-circuit condition. As stated above, the electric charge induced by piezoelectricity has the same sign on both surfaces, and only flexoelectricity contributes to the current flow. However, the peak output charge rapidly decreases to 0.075 pC when the beam thickness reduces to one micrometer, which is hard to measure practically. This phenomenon can also be directly explained by the static solution of the output charge,

$$Q = \frac{3\mu_{31}bh}{40L} = \frac{3\mu_{31}h}{20\beta}. \quad (47)$$

The results above give us a new understanding of measuring the flexoelectric coefficients, that is, to get detectable electric charge output, the beam size should be avoided to made too small. Moreover, we introduce

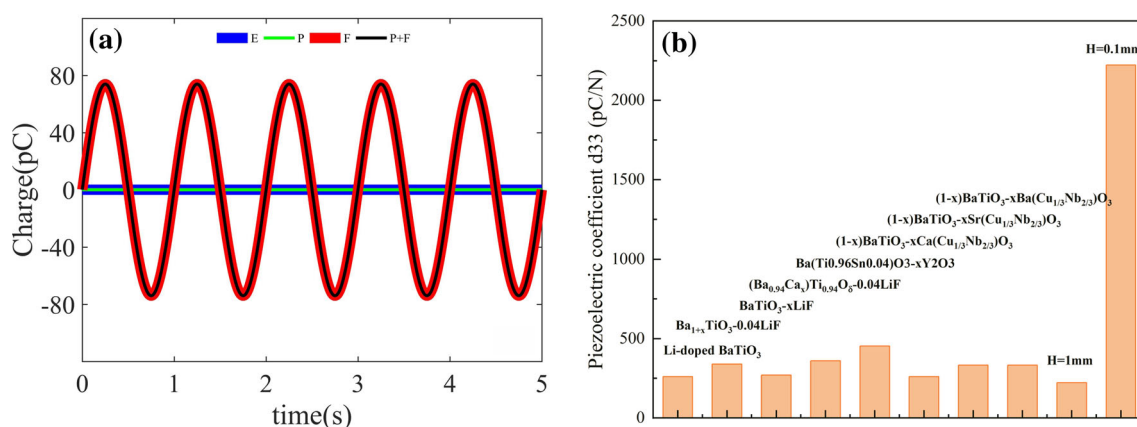


**Fig. 4** **a** Dynamic output charge versus time with  $H = 1$  mm,  $\beta = 20$ ; **b** piezoelectric coefficient  $d_{33}$  of doped BT [58] and effective piezoelectric coefficient  $d_{33}^{\text{eff}}$  of an Euler–Bernoulli flexoelectric beam

the effective piezoelectric coefficient, which can be expressed as

$$d_{33}^{\text{eff}} = \frac{6\mu_{31}\beta^2}{Eh}. \quad (48)$$

We can see that the coefficient is inversely proportional to the beam thickness; hence, it can be significantly enhanced when the beam thickness decreases to microscale, as illustrated in Fig. 4b. The toxicity and environmental impacts of lead have shifted the attention from the most widely used lead zirconate titanate piezoceramics to alkaline bismuth titanate-based piezoelectric ceramics. Chemical modification or microstructurally engineering BT-based materials have been fabricated and selected to substitute for lead zirconate titanate piezoceramics. As compared in Fig. 4b, the effective piezoelectric coefficient  $d_{33}$  (222 pC/N) is comparable with the piezoelectric-doped BT (largest value, 454 pC/N) when the beam thickness is at one millimeter; however, the effective piezoelectric coefficient  $d_{33}$  (2222 pC/N) will be much stronger than that of the piezoelectric doped BT ceramics. Furthermore, the effective piezoelectric coefficient  $d_{33}$  is size dependent of the beam thickness; this gives a novel way to design piezoelectric materials by flexoelectricity.

## 6 Conclusions

This work presents the forced vibration of a piezoelectric and flexoelectric Euler–Bernoulli beam by the Green’s function solution. The exact solutions for the harmonically excited beams are derived for cantilevers with different beam thicknesses. The tip deflection, dynamic output voltage, and dynamic output charge were selected to demonstrate the effect of the flexoelectric effect. Numerical results for BaTiO<sub>3</sub> cantilevers showed that the tip deflection would be smaller than that predicted by the classical piezoelectric beam theory. The dynamic output voltage and charge are negligible when the beam thickness reduces to microscale; however, several methods are proposed here to effectively enhance the electric response, such as changing the length–thickness ratio or introduce the effective piezoelectric coefficients. Our results imply that pure mechanical experiments can be used to determine the flexoelectric effect with different electrical boundary conditions. Moreover, our results showed that mechanical structural design can be another novel way to fabricate BT-based piezoelectric materials with ultrahigh piezoelectric coefficient.

**Acknowledgements** The authors sincerely appreciate the financial support by the National Natural Science Foundation of China (No. 11602189, 11672222, 12072251), The Chang Jiang Scholar Program and Project B18040. Xu also thanks to the financial support by the Key Laboratory for Intelligent Nano Materials and Devices of the Ministry of Education (INMD-2020M08).

**Compliance with ethical standards**

**Conflict of interest** The authors declare that they have no known competing financial interests or personal relationships that could have appeared to influence the work reported in this paper.

## References

1. Eom, C., Troliermckinstry, S.: Thin-film piezoelectric MEMS. *MRS Bull.* **37**(11), 1007–1017 (2012)
2. Lee, D., Yang, S.M., Yoon, J., Noh, T.W.: Flexoelectric rectification of charge transport in strain-graded dielectrics. *Nano Lett.* **12**(12), 6436–6440 (2012)
3. Bhaskar, U.K., Banerjee, N., Abdollahi, A., Wang, Z., Schlom, D.G., Rijnders, G., Catalan, G.: A flexoelectric microelectromechanical system on silicon. *Nat. Nanotechnol.* **11**(3), 263 (2016)
4. Narvaez, J., Vasquezsancho, F., Catalan, G.: Enhanced flexoelectric-like response in oxide semiconductors. *Nature* **538**(7624), 219 (2016)
5. Liang, X., Hu, S.L., Shen, S.P.: Nanoscale mechanical energy harvesting using piezoelectricity and flexoelectricity. *Smart Mater. Struct.* **26**(3), 035050 (2017)
6. Ma, W.H., Cross, L.E.: Large flexoelectric polarization in ceramic lead magnesium niobate. *Appl. Phys. Lett.* **79**(26), 4420–4422 (2001)
7. Ma, W.H., Cross, L.E.: Flexoelectric polarization of barium strontium titanate in the paraelectric state. *Appl. Phys. Lett.* **81**(18), 3440–3442 (2002)
8. Ma, W.H., Cross, L.E.: Flexoelectric effect in ceramic lead zirconate titanate. *Appl. Phys. Lett.* **86**(7), 072905 (2005)
9. Ma, W.H., Cross, L.E.: Flexoelectricity of barium titanate. *Appl. Phys. Lett.* **88**(23), 232902 (2006)
10. Askar, A., Lee, P., Cakmak, A.S.: Lattice-dynamics approach to the theory of elastic dielectrics with polarization gradient. *Phys. Rev. B* **1**(8), 3525 (1970)
11. Tagantsev, A.K.: Piezoelectricity and flexoelectricity in crystalline dielectrics. *Phys. Rev. B* **34**(8), 5883 (1986)
12. Hong, J.W., Vanderbilt, D.: The flexoelectricity of barium and strontium titanates from first principles. *J. Phys. Condens. Matter.* **22**(11), 112201 (2010)
13. Hong, J.W., Vanderbilt, D.: First-principles theory and calculation of flexoelectricity. *Phys. Rev. B* **88**(17), 174107 (2013)
14. Mindlin, R.D.: Micro-structure in linear elasticity. *Arch. Ration. Mech. Anal.* **16**(1), 51–78 (1964)
15. Mindlin, R.D., Eshel, N.N.: On first strain-gradient theories in linear elasticity. *Int. J. Solids Struct.* **4**(1), 109–124 (1968)
16. Toupin, R.A.: Theories of elasticity with couple-stress. *Arch. Ration. Mech. Anal.* **17**(2), 85–112 (1964)
17. Eringen, A.C.: Linear theory of nonlocal elasticity and dispersion of plane waves. *Int. J. Solids Struct.* **10**(5), 425–435 (1972)
18. Eringen, A.C., Edelen, D.: On nonlocal elasticity. *Int. J. Eng. Sci.* **10**(3), 233–248 (1972)
19. Mindlin, R.D.: Polarization gradient in elastic dielectrics. *Int. J. Solids Struct.* **4**(6), 637–642 (1968)
20. Sharma, N., Maranganti, R., Sharma, P.: On the possibility of piezoelectric nanocomposites without using piezoelectric materials. *J. Mech. Phys. Solids* **55**(11), 2328–2350 (2007)
21. Majdoub, M., Sharma, P., Cagin, T.: Enhanced size-dependent piezoelectricity and elasticity in nanostructures due to the flexoelectric effect. *Phys. Rev. B* **77**(12), 125424 (2008)
22. Majdoub, M., Sharma, P., Cagin, T.: Dramatic enhancement in energy harvesting for a narrow range of dimensions in piezoelectric nanostructures. *Phys. Rev. B* **78**(12), 121407 (2008)
23. Sharma, N.D., Landis, C.M., Sharma, P.: Piezoelectric thin-film superlattices without using piezoelectric materials. *J. Appl. Phys.* **108**(2), 024304 (2010)
24. Deng, Q., Kammoua, M., Erturk, A., Sharma, P.: Nanoscale flexoelectric energy harvesting. *Int. J. Solids Struct.* **51**(18), 3218–3225 (2014)
25. Hu, S.L., Shen, S.P.: Electric field gradient theory with surface effect for nano-dielectrics. *CMC-Comput. Mater. Contin.* **13**(1), 63 (2009)
26. Hu, S.L., Shen, S.P.: Variational principles and governing equations in nano-dielectrics with the flexoelectric effect. *Sci. China Phys. Mech. Astron.* **53**(8), 1497–1504 (2010)
27. Shen, S.P., Hu, S.L.: A theory of flexoelectricity with surface effect for elastic dielectrics. *J. Mech. Phys. Solids* **58**(5), 665–677 (2010)
28. Yan, Z., Jiang, L.Y.: Flexoelectric effect on the electroelastic responses of bending piezoelectric nanobeams. *J. Appl. Phys.* **113**(19), 194102 (2013)
29. Yan, Z., Jiang, L.Y.: Size-dependent bending and vibration behaviour of piezoelectric nanobeams due to flexoelectricity. *J. Phys. D Appl. Phys.* **46**(35), 355502 (2013)
30. Zhang, Z.R., Jiang, L.Y.: Size effects on electromechanical coupling fields of a bending piezoelectric nanoplate due to surface effects and flexoelectricity. *J. Appl. Phys.* **116**(13), 134308 (2014)
31. Liang, X., Hu, S.L., Shen, S.P.: Effects of surface and flexoelectricity on a piezoelectric nanobeam. *Smart Mater. Struct.* **23**(3), 035020 (2014)
32. Liang, X., Hu, S.L., Shen, S.P.: Size-dependent buckling and vibration behaviors of piezoelectric nanostructures due to flexoelectricity. *Smart Mater. Struct.* **24**(10), 105012 (2015)
33. Liang, X., Yang, W.J., Hu, S.L., Shen, S.P.: Buckling and vibration of flexoelectric nanofilms subjected to mechanical loads. *J. Phys. D Appl. Phys.* **49**(11), 115307 (2016)
34. Yan, Z.: Size-dependent bending and vibration behaviors of piezoelectric circular nanoplates. *Smart Mater. Struct.* **25**(3), 035017 (2016)
35. Moura, A.G., Erturk, A.: Size effects in piezoelectric cantilevers at submicron thickness levels due to flexoelectricity. *Proc. SPIE* **10164**, 1016405 (2017)
36. Lurie, S., Solyaev, Y.: On the formulation of elastic and electroelastic gradient beam theories. *Contin. Mech. Thermodyn.* **31**, 1–13 (2019)
37. Zhang, C.L., Zhang, L.L., Shen, X.D., Chen, W.Q.: Enhancing magnetoelectric effect in multiferroic composite bilayers via flexoelectricity. *J. Appl. Phys.* **119**(13), 134102 (2016)
38. Chu, Z.Q., PourhosseiniAsl, M., Dong, S.X.: Review of multi-layered magnetoelectric composite materials and devices applications. *J. Phys. D Appl. Phys.* **51**(24), 243001 (2018)
39. Hana, P.: Study of flexoelectric phenomenon from direct and from inverse flexoelectric behavior of PMNT ceramic. *Ferroelectrics* **351**(1), 196–203 (2007)

40. Abuhilal, M.: Forced vibration of Euler–Bernoulli beams by means of dynamic Green functions. *J. Sound Vib.* **267**(2), 191–207 (2003)
41. Li, X.Y., Zhao, X., Li, Y.H.: Green’s functions of the forced vibration of Timoshenko beams with damping effect. *J. Sound Vib.* **333**(6), 1781–1795 (2014)
42. Chu, B.J., Salem, D.R.: Flexoelectricity in several thermoplastic and thermosetting polymers. *Appl. Phys. Lett.* **101**(10), 103905 (2012)
43. Poddar, S., Ducharme, S.: Measurement of the flexoelectric response in ferroelectric and relaxor polymer thin films. *Appl. Phys. Lett.* **103**(20), 202901 (2013)
44. Lu, J.F., Lv, J.Y., Liang, X., Xu, M.L., Shen, S.P.: Improved approach to measure the direct flexoelectric coefficient of bulk polyvinylidene fluoride. *J. Appl. Phys.* **119**(9), 094104 (2016)
45. Liu, J., Zhou, Y., Hu, X.P., Chu, B.J.: Flexoelectric effect in PVDF-based copolymers and terpolymers. *Appl. Phys. Lett.* **112**(23), 232901 (2018)
46. Mbarki, R., Baccam, N., Dayal, K., Sharma, P.: Piezoelectricity above the Curie temperature? Combining flexoelectricity and functional grading to enable high-temperature electromechanical coupling. *Appl. Phys. Lett.* **104**(12), 122904 (2014)
47. Chu, L.L., Li, Y.B., Dui, G.S.: Size-dependent electromechanical coupling in functionally graded flexoelectric nanocylinders. *Acta Mech.* **230**(9), 3071–3086 (2019)
48. Qi, L.: Energy harvesting properties of the functionally graded flexoelectric microbeam energy harvesters. *Energy* **171**, 721–730 (2019)
49. Chu, L.L., Li, Y.B., Dui, G.S.: Nonlinear analysis of functionally graded flexoelectric nanoscale energy harvesters. *Int. J. Mech. Sci.* **167**, 105282 (2020)
50. Yang, W.J., Liang, X., Shen, S.P.: Electromechanical responses of piezoelectric nanoplates with flexoelectricity. *Acta Mech.* **226**(9), 3097–3110 (2015)
51. Zhang, R.Z., Liang, X., Shen, S.P.: A Timoshenko dielectric beam model with flexoelectric effect. *Meccanica* **51**(5), 1181–1188 (2016)
52. Tiersten, H.: Hamilton’s principle for linear piezoelectric media. *Proc. IEEE* **55**(8), 1523–1524 (1967)
53. Liang, X., Shen, S.P.: Size-dependent piezoelectricity and elasticity due to the electric field-strain gradient coupling and strain gradient elasticity. *Int. J. Appl. Mech.* **05**(02), 1350015 (2013)
54. Liang, X., Hu, S.L., Shen, S.P.: Bernoulli–Euler dielectric beam model based on strain-gradient effect. *J. Appl. Mech.* **80**(4), 044502 (2013)
55. Park, K., Xu, S., Liu, Y., Hwang, G., Kang, S.L., Wang, Z.L., Lee, K.J.: Piezoelectric BaTiO<sub>3</sub> thin film nanogenerator on plastic substrates. *Nano Lett.* **10**(12), 4939–4943 (2010)
56. Koka, A., Zhou, Z., Sodano, H.A.: Vertically aligned BaTiO<sub>3</sub> nanowire arrays for energy harvesting. *Energy Environ. Sci.* **7**(1), 288–296 (2014)
57. Fan, F., Tang, W., Wang, Z.L.: Flexible nanogenerators for energy harvesting and self-powered electronics. *Adv. Mater.* **28**(22), 4283–4305 (2016)
58. Acosta, M., Novak, N., Rojas, V., Patel, S., Vaish, R., Koruza, J., Rossetti, G.A., Rodel, J.: BaTiO<sub>3</sub>-based piezoelectrics: Fundamentals, current status, and perspectives. *Appl. Phys. Lett.* **4**(4), 041305 (2017)